informa
healthcare

REVIEW

Imaging of the Lamina Cribrosa in Glaucoma: Perspectives of Pathogenesis and Clinical Applications*

Tae-Woo Kim[1], Larry Kagemann[2], Michaël J. A. Girard[3,4], Nicholas G. Strouthidis[4,5], Kyung Rim Sung[6], Christopher K. Leung[7], Joel S. Schuman[2] and Gadi Wollstein[2]

[1]Department of Ophthalmology, Seoul National University Bundang Hospital, Seoul National University College of Medicine, Seoul, Republic of Korea, [2]UPMC Eye Center, Eye and Ear Institute, Ophthalmology and Visual Science Research Center, Department of Ophthalmology, University of Pittsburgh School of Medicine, Pittsburgh, PA, USA, [3]Department of Bioengineering, National University of Singapore, Singapore, [4]Singapore Eye Research Institute, Singapore, [5]NIHR Biomedical Research Centre at Moorfields Eye Hospital NHS Foundation Trust and UCL Institute of Ophthalmology, London, UK, [6]Department of Ophthalmology, University of Ulsan, College of medicine, Asan Medical Center, Seoul, Republic of Korea, and [7]Department of Ophthalmology and Visual Sciences, The Chinese University of Hong Kong, Hong Kong, China

ABSTRACT

The lamina cribrosa (LC) is a sieve-like structure in the sclera where retinal ganglion cell axons exit from the eye. The LC has been known to play a critical role in the pathogenesis of glaucoma. With the advent of imaging technologies, such as enhanced depth imaging, spectral-domain optical coherence tomography (OCT) enables us to unveil the LC *in vivo* features. The application of adaptive optics technology and a compensatory image-processing algorithm has further improved the visualization of the beams and pores and neural pathways of the LC and the scleral insertion sites. Monitoring the changes of these structures in relation to acute and chronic elevation of intraocular pressure would be germane to decipher the relationship between the stress and strain response of the LC and optic nerve damage and improve our understanding of glaucoma pathophysiology. While the impact of investigating the integrity of LC is substantive, considerable challenges remain for imaging the LC. Nevertheless, with the rapid development of the OCT technology, it is expected that some of these limitations can be overcome and the potentials of LC imaging will be unraveled.

Keywords: Glaucoma, intraocular pressure, lamina cribrosa, optical coherence tomography

INTRODUCTION

The lamina cribrosa (LC) is a multi-layered sieve-like structure in the sclera where retinal ganglion cell axons exit from the eye. The LC has been known to play a critical role in the pathogenesis of glaucoma.[1] Blockage of axonal transport within the LC has been proposed as a salient pathogenic mechanism for glaucoma.[2,3] However, the exact process of the pathogenic cascade within the LC is yet to be determined. In clinical practice, assessment of the glaucomatous damage is performed by examining the optic nerve head (ONH) and its surroundings for signs of structural loss, such as neuroretinal rim loss or enlarged cupping. Remodeling of the LC within the ONH has been

RIGHTS LINK

shown to be associated with glaucomatous structural damage.[4–6]

Strong evidence also suggests that the biomechanics of the ONH connective tissues (LC and sclera) may dictate the intraocular pressure (IOP) level that can be safely sustained. Above an individual-specific IOP threshold, the LC could exhibit non-homeostatic deformations (induced by IOP), which could result in altered blood flow and axonal transport, diminished oxygen/nutrient supply, negative mechanotransduction (the mechanism by which cells convert mechanical stimuli to chemical signals), and thus vision loss. Key biomechanical factors of the ONH include, but are not limited to, LC elastin/collagen fiber organization, LC morphology, and LC stiffness. In vivo measurements of such factors, using ocular imaging, could prove critical for our understanding of ONH physiology and glaucoma pathophysiology.

Unfortunately, the entire LC is rarely visible in routine ophthalmoscopic examination due to the prelaminar neuroretinal tissue. Even in some far advanced glaucomatous eyes where little remnant prelaminar tissue exists, only the anterior surface of the LC is visible with deeper portions of the LC observable only by histologic sectioning. Optical coherence tomography (OCT), an ocular imaging device, can provide high resolution cross-sectional images of the ONH in vivo.[7] However, due to the typical signal attenuation of OCT signal as it is penetrating into deep structures, deep-seated structures such as the LC are difficult to visualize with this technology. Recent improvements in imaging technologies, including enhanced depth imaging (EDI) and sophisticated analyzing techniques, enable unveiling of the LC in vivo features.[8–19] Optic nerve acquires myelination in retrolaminar region and thus its diameter abruptly expands to approximately twice that of the disc. The line of myelination would seem the histologic posterior boundary of the lamina and its visualization the goal of OCT.

This article summarizes a Special Interest Group session conducted during the 2012 Association for Research in Vision and Ophthalmology meeting to discuss the current status and future directions of OCT imaging of the LC.

ULTRAHIGH-RESOLUTION SD-OCT IMAGING OF THE LC

Successful visualization of the LC in the clinical setting is now possible by using OCT, though the quality of imagery depends on the individual eye, the technique used during acquisition, and the imaging platform used.

Visualization of LC pores is possible by disc photography in some eyes.[20] Best SD-OCT visualization of the LC occurs when pores are visible in disc photos. LC imaging requires a focal plane positioned posterior to the retinal surface, known as EDI. The best LC visualization is obtained by maximizing the sharpness of the cross-sectional image of the laminar beams. Preferably, A-scan spacing should equal B-scan spacing, with the highest density allowed by the scanner. This isometric sampling of the tissue allows for comprehensive post-processing analysis of the lamina. It should be remembered that longer scans are prone to increased eye movement. Non-compliant subjects may require faster, lower density scans, resulting in poorer visualization of structure.

All commercially available SD-OCT devices are limited to a transverse resolution of $\sim$20 μm, yielding blurred images of LC pores. In 2009, Torti et al.[21] published the first images of the LC obtained with an OCT equipped with adaptive optics. Engaging adaptive optics techniques to OCT led to improved transverse resolution from 20 to 4 μm, improving the visualization of laminar beams (Figure 1). Acquiring volumetric image data of the LC enables isolation and displaying the space within the pores (Figure 2). Isolation of these pathways provides a new family of measurement parameters describing the morphology of the nerve bundles and glial tissues such as LC neural volume, pathway tortuosity, the distribution of pathway diameters, frequency of pathway branch points, etc.

In summary, visualization of the beams and pores of the LC can be accomplished with commercially available SD-OCT devices. The addition of adaptive optics yields imagery useful for rudimentary quantitative assessment. Application of advanced post-processing allows a unique visualization of the pore space, providing deeper understanding of the morphology of the nerve bundles as they traverse the LC.

IMPROVING DETECTION OF THE LC

The image quality of commercial OCT devices has drastically improved and is now sufficient to visualize deep connective tissue structures such as the LC and the posterior sclera – both of which are thought to be important biomechanical players in ocular disorders such as glaucoma, myopia and papilledema.[10,11,14] However, OCT image quality is still inferior to that of histology, which is a major limitation for clinical hypothesis testing using OCT. Specifically, in most subjects, the LC is only partially detectable even with recent hardware improvement techniques such as EDI.[22] The partial visibility of the LC is due to light attenuation. This limits the visualization of the anterior, and especially the posterior, boundaries of the LC and the detection of the LC insertion into the peripapillary sclera. Moreover, when light attenuation is too strong, shadows, usually casted by blood
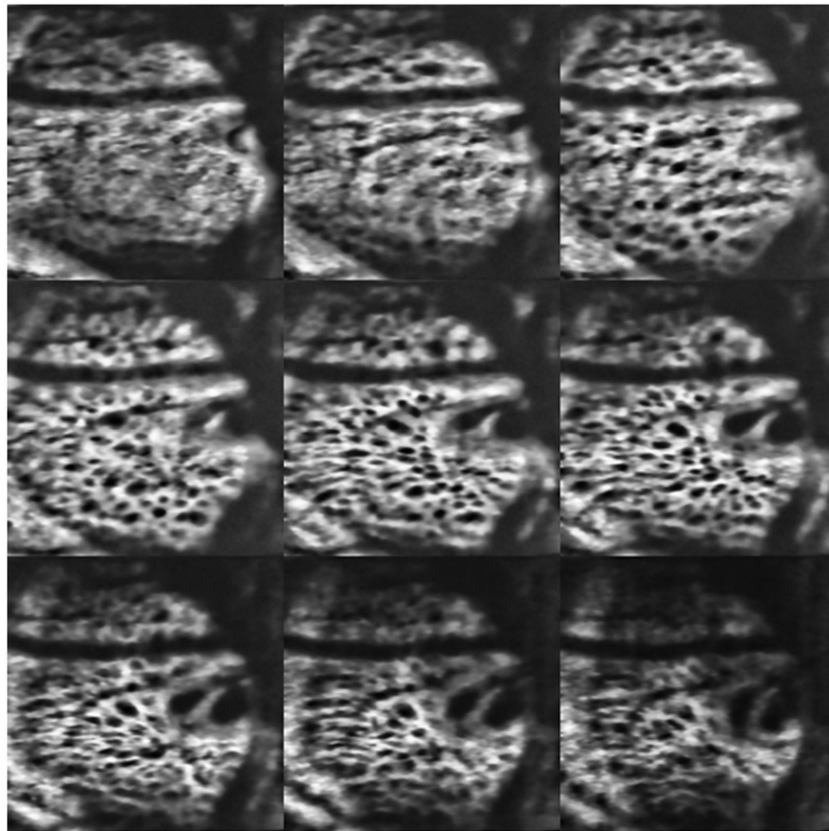
FIGURE 1 A series of coronal slices of the LC, extending from the anterior (upper left) to the posterior (lower right) was obtained in a healthy living subject by adaptive optics SD-OCT.
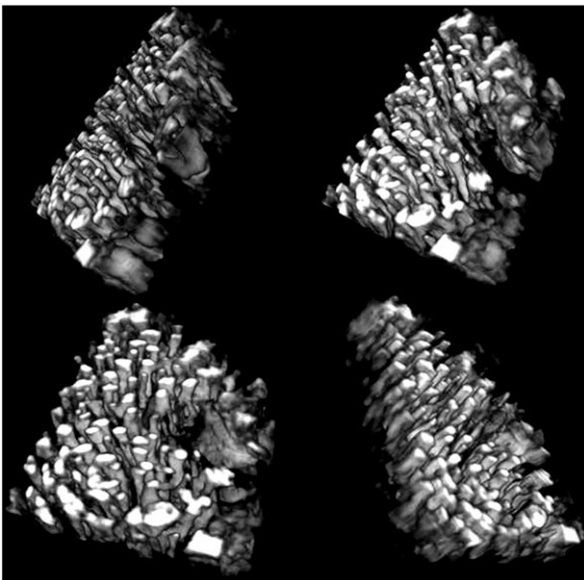
FIGURE 2 The clear visualization of the pore space demonstrated in Figure 1 permits 3D visualization of that space, allowing appreciation and measurement of the paths, volume, and tortuosity neural pathways through the LC. Pores appear as round elongated structures.

vessels from the central retinal trunk, are created which further limit proper LC detection.

To improve detection of the LC in OCT images, one needs to incorporate the physical properties of light

attenuation in the OCT technology in order to correct for such effects. By adapting and improving compensation techniques that were originally developed for ultrasound imaging we were able to drastically enhance OCT images of ONH.[12,23,24] Specifically, these techniques can (1) improve the visibility of LC/sclera insertion sites (Figure 3); (2) improve the visibility of focal LC defects (Figure 4); (3) drastically improve contrast across all tissue boundaries (especially the anterior LC boundary; Figures 3 and 4); (4) remove blood vessel shadows in the ONH tissues (Figures 3 and 4); (5) help identify the full thickness of the LC (data not shown); and (6) improve the visibility of the peripapillary choroid and sclera (Figures 3 and 4). These compensation techniques, when combined with EDI, provide the best LC detection.[25] Although only one SD-OCT (Spectralis, Heidelberg Engineering, Heidelberg, Germany) has been tested here, the proposed techniques can also be applied to time-domain, swept-source and adaptive optics OCT.

In summary, we have demonstrated that OCT image quality can be improved using relatively simple image processing that can correct for light attenuation. These techniques are further refined in order to limit noise over-amplification and to provide a better integration with OCT hardware. It should be emphasized that not all of the above improvements
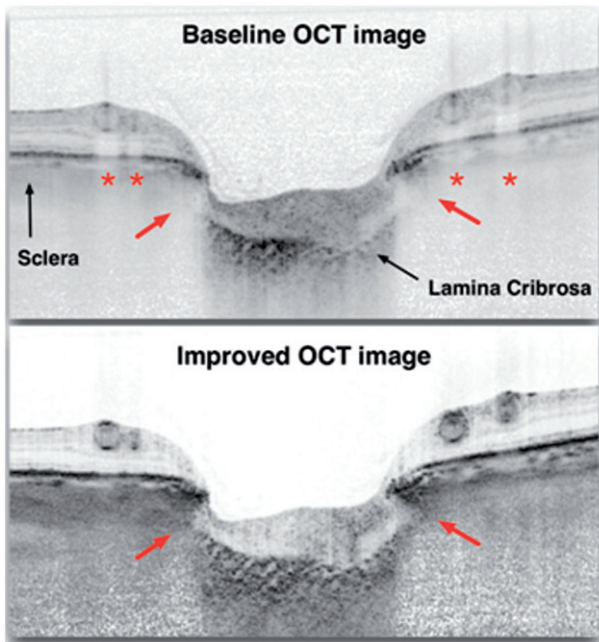
FIGURE 3 Improved visibility of the LC/sclera insertion sites (arrows) by the compensation algorithm. Note that the contrast of the anterior LC is improved and blood vessel shadows (asterisks) are corrected. Similarly, the visibility of the peripapillary sclera and the choroidal contrast are improved. (OCT image courtesy of Sean Sung Chul Park, MD, from the New York Eye and Ear Infirmary, New York, NY).

FIGURE 4 Visualization of poorly detected focal lamina defects (arrow) were enhanced by using compensation algorithms. Note the contrast of the anterior LC boundary is improved and blood vessel shadows (asterisks) are corrected. (OCT image courtesy of Sean Sung Chul Park, MD, from the New York Eye and Ear Infirmary, New York, NY).

can be achieved in every eye, and care must be taken for data interpretation.

IMAGING THE LC IN GLAUCOMA: EXPERIMENTAL STUDIES

In tandem with clinical SD-OCT imaging studies of the LC, important work has been conducted in experimental animal models that serve to inform future studies in human subjects. Most experimental work has been conducted in the rhesus macaque, as this animal's LC closely resembles that of the human. The pig also has a robust connective tissue LC and so has been adopted by other investigators.[26,27] The first "proof" that SD-OCT could detect the LC came from a detailed histologic comparison using a normal rhesus macaque eye, imaged *in vivo* by SD-OCT at IOP 10 mmHg and then sacrificed with IOP also fixed at 10 mmHg.[28] The anterior surface of the LC was reliably detected within ONH B-scans but the posterior surface, and therefore the full thickness of the LC, were not reliably detected. A subsequent study undertaken in rhesus macaques demonstrated that EDI improved detection of what is assumed to be the posterior LC surface both in normal and experimental glaucoma eyes.[17] The detection of the posterior LC surface, however, has not yet been verified by comparison to histology in the human or non-human primate eye. Histologic studies conducted on porcine eyes, albeit

imaged *ex vivo*, suggest that the full thickness of the LC can be captured in this animal.[27] However, as the posterior termination of LC "signal" can be highly variable in humans, measurement of LC "thickness" by SD-OCT should be interpreted with caution until further validation studies are available.

The effect of chronic IOP elevation has been examined in nine adult rhesus macaques in which one eye underwent IOP elevation by sequential laser insults to the trabecular meshwork and in which the fellow eye acted as a normal control.[28] This study demonstrated that SD-OCT was capable of detecting longitudinal ONH structural changes in response to chronic experimental IOP elevation. Specifically, thinning of pre-laminar tissue, reduction of "minimum rim width", posterior displacement of Bruch's membrane opening (BMO) and posterior displacement of the anterior LC surface were all detected (Figure 5). Furthermore, these changes all occurred prior to the detection of peripapillary nerve fiber layer thinning by SD-OCT. SD-OCT imaging in the monkey model of glaucoma may also be augmented using adaptive optics scanning laser ophthalmoscopy that can detect changes in laminar pore morphology induced by experimental glaucoma.[29] It is likely that LC imaging will play a role in longitudinal clinical imaging of subjects with, or at risk of, glaucoma, but as yet it remains uncertain how the structural changes detected might relate to future functional damage.

Although the effect of acute IOP manipulation in human subjects has been investigated *in vivo* using
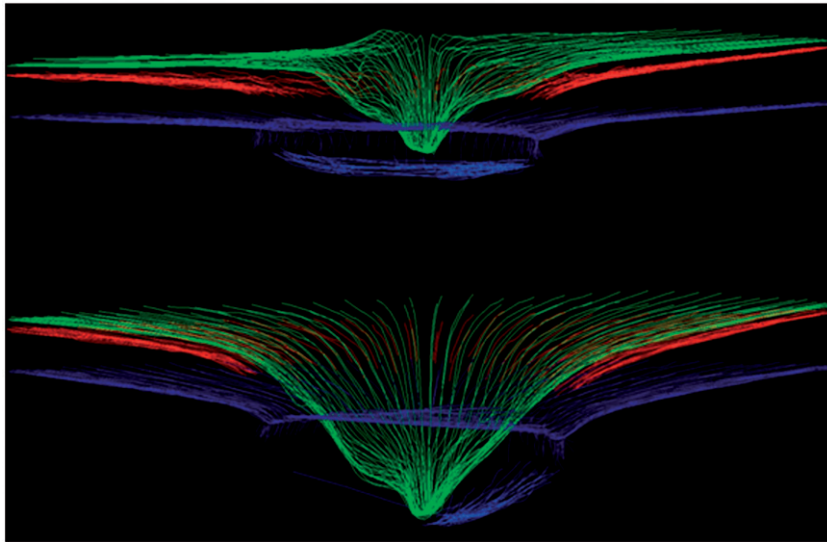
FIGURE 5 The effect of chronic IOP elevation upon the rhesus macaque ONH as imaged by SD-OCT. The upper image was acquired at baseline, and the lower image was acquired 8 months after laser treatment to the trabecular meshwork. The structures delineated are the internal limiting membrane (green, first line), the posterior surface of the retinal nerve fiber layer (red, second line), Bruch's membrane/retinal pigment epithelium and border tissue (dark blue, third line) and the anterior LC surface (light blue, bottom line). Note the profound posterior displacement of the internal limiting membrane and the surface of the lamina in the lower figure.

ophthalmodynamometry,[30] animal models may be used to achieve a more controlled and sustained IOP perturbation. In a study of 10 normal rhesus macaque eyes, SD-OCT imaging was performed at IOP 10 mmHg (stabilized for 30 min) and at IOP 45 mmHg (stabilized for 60 min), using a manometer and reservoir connected via a cannula into the anterior chamber of the imaged eye.[16] Significant decreases in prelaminar tissue but not nerve fiber layer thickness were detected with IOP elevation, as in the human study. Unlike the human eyes, significant posterior displacement of BMO (perhaps reflecting underlying peripapillary scleral deformation) and, in two eyes, significant posterior displacement of the anterior LC surface were also detected.

These findings confirm that SD-OCT is capable of detecting changes in the LC in response to acute IOP changes. An ability to measure such deformations is a crucial first step in characterizing ONH biomechanics *in vivo*.

IMAGING THE LC IN GLAUCOMA: A CLINICAL STUDY

Lowering IOP has been the mainstay of glaucoma treatment. However, little has been known about the effect of IOP lowering in the deep optic nerve, especially in the LC, which is the putative primary site of axonal injury in glaucoma. Lee et al.[19] used SD-OCT to investigate the response of the LC and prelaminar tissue to the IOP lowering effect of glaucoma surgery and to determine the factors influencing such responses. Thirty-five primary open-angle glaucoma patients who underwent trabeculectomy were imaged with the SD-OCT EDI protocol before surgery, 1 week after surgery, and 1, 3 and 6 months postoperatively. The pre- and postoperative magnitude of the LC displacement and the thickness of LC and prelaminar tissue were determined on multiple B-scan images in each eye. There was a significant IOP reduction from the preoperative level of 27.2 ± 8.9–10.5 ± 3.4 mmHg at the 6 months visit postoperatively. At the same time, the amount of posterior displacement of the LC was significantly decreased from a mean preoperative level of 614.6 ± 179.6 to 503.9 ± 142.7 µm 6 months after operation. Significant thickening of the LC and prelaminar tissue were observed at postoperative 6 months. They also reported that the magnitude of reduction in LC displacement was significantly associated with younger age, greater percent IOP reduction and greater preoperative LC displacement. However, the amount of LC and prelaminar thickening was not associated with any of the factors.

This study demonstrated a significant reduction in the posterior displacement and increase in the thickness of the LC and prelaminar tissue in patients who received glaucoma surgery using EDI SD-OCT of the ONH. The importance and influence of the reversal of LC displacement on glaucoma prognosis remains to be determined. However, based on the current understanding of the role of LC displacement in the pathogenesis of glaucomatous damage (i.e. backward bowing of the LC may cause mechanical or vascular damage to the ganglion cell axons),[31] it may be proposed that reversal of LC displacement might be a sign of released strain at the level of the LC, which may give relief to the compressed nerve fibers or laminar capillaries. Further study is needed to

determine the influence of the reversal of LC displacement after IOP reduction on disease prognosis.

CONCLUSIONS

The advent of OCT imaging has facilitated the visualization of the LC, providing mechanistic insights into the development and progression of glaucoma. Although the LC can only be partially detected in most commercially available SD-OCT instruments, the application of adaptive optics technology and a compensatory image-processing algorithm has improved the visualization of the beams and pores and neural pathways of the LC and the scleral insertion sites. Monitoring the changes of these structures in relation to acute and chronic elevation of IOP would be germane to decipher the relationship between the stress and strain response of the LC and optic nerve damage. While the impact of investigating the integrity of LC is substantive, considerable challenges remain for imaging the LC. Axonal bundles, glial cells and small capillaries within the beams might have an important role in the susceptibility to diseases and its progression but cannot be visualized and quantified directly. Retinal blood vessels and the neuroretinal rim can obscure the LC and the detection of the posterior LC surface and measurement of LC thickness often is difficult. Validating tissue reflectivity in the OCT images is challenging because correspondence in tissue structure and architecture between *in vivo* images and histologic sections can be hard to attain. Nevertheless, with the rapid development of ultrahigh-resolution OCT imaging technologies, it is expected that some of these limitations can be overcome and the potentials of LC imaging will be unraveled.

DECLARATION OF INTEREST

REFERENCES

1. Quigley HA, Addicks EM, Green WR, Maumenee AE. Optic nerve damage in human glaucoma. II. The site of injury and susceptibility to damage. Arch Ophthalmol 1981;99:635–649.
2. Quigley HA, Anderson DR. Distribution of axonal transport blockade by acute intraocular pressure elevation in the primate optic nerve head. Invest Ophthalmol Vis Sci 1977;16:640–644.
3. Radius RL, Anderson DR. Rapid axonal transport in primate optic nerve. Distribution of pressure-induced interruption. Arch Ophthalmol 1981;99:650–654.
4. Bellezza AJ, Rintalan CJ, Thompson HW, Downs JC, Hart RT, Burgoyne CF. Deformation of the lamina cribrosa and anterior scleral canal wall in early experimental glaucoma. Invest Ophthalmol Vis Sci 2003;44:623–637.
5. Quigley HA, Hohman RM, Addicks EM, Massof RW, Green WR. Morphologic changes in the lamina cribrosa correlated with neural loss in open-angle glaucoma. Am J Ophthalmol 1983;95:673–691.
6. Yang H, Downs JC, Girkin C, Sakata L, Bellezza A, Thompson H, Burgoyne CF. 3-D histomorphometry of the normal and early glaucomatous monkey optic nerve head: lamina cribrosa and peripapillary scleral position and thickness. Invest Ophthalmol Vis Sci 2007;48: 4597–4607.
7. Huang D, Swanson EA, Lin CP, Schuman JS, Stinson WG, Chang W, et al. Optical coherence tomography. Science 1991;254:1178–1181.
8. Srinivasan VJ, Adler DC, Chen Y, Gorczynska I, Huber R, Duker JS, et al. Ultrahigh-speed optical coherence tomography for three-dimensional and en face imaging of the retina and optic nerve head. Invest Ophthalmol Vis Sci 2008;49:5103–5110.
9. Inoue R, Hangai M, Kotera Y, Nakanishi H, Mori S, Morishita S, Yoshimura N. Three-dimensional high-speed optical coherence tomography imaging of lamina cribrosa in glaucoma. Ophthalmology 2009;116:214–222.
10. Kagemann L, Ishikawa H, Wollstein G, Brennen PM, Townsend KA, Gabriele ML, Schuman JS. Ultrahigh-resolution spectral domain optical coherence tomography imaging of the lamina cribrosa. Ophthalmic Surg Lasers Imaging 2008;39:S126–S131.
11. Strouthidis NG, Grimm J, Williams GA, Cull GA, Wilson DJ, Burgoyne CF. A comparison of optic nerve head morphology viewed by spectral domain optical coherence tomography and by serial histology. Invest Ophthalmol Vis Sci 2010;51:1464–1474.
12. Girard MJ, Strouthidis NG, Ethier CR, Mari JM. Shadow removal and contrast enhancement in optical coherence tomography images of the human optic nerve head. Invest Ophthalmol Vis Sci 2011;52:7738–7748.
13. Lee EJ, Kim TW, Weinreb RN, Park KH, Kim SH, Kim DM. Visualization of the lamina cribrosa using enhanced depth imaging spectral-domain optical coherence tomography. Am J Ophthalmol 2011;152:87–95.e81.
14. Park SC, De Moraes CG, Teng CC, Tello C, Liebmann JM, Ritch R. Enhanced depth imaging optical coherence tomography of deep optic nerve complex structures in glaucoma. Ophthalmology 2012;119:3–9.

15. Park HY, Jeon SH, Park CK. Enhanced depth imaging detects lamina cribrosa thickness differences in normal tension glaucoma and primary open-angle glaucoma. Ophthalmology 2012;119:10–20.

16. Strouthidis NG, Fortune B, Yang H, Sigal IA, Burgoyne CF. Effect of acute intraocular pressure elevation on the monkey optic nerve head as detected by spectral domain optical coherence tomography. Invest Ophthalmol Vis Sci 2011;52:9431–9437.

17. Yang H, Qi J, Hardin C, Gardiner SK, Strouthidis NG, Fortune B, Burgoyne CF. Spectral-domain optical coherence tomography enhanced depth imaging of the normal and glaucomatous nonhuman primate optic nerve head. Invest Ophthalmol Vis Sci 2012;53:394–405.

18. Park SC, Kiumehr S, Teng CC, Tello C, Liebmann JM, Ritch R. Horizontal central ridge of the lamina cribrosa and regional differences in laminar insertion in healthy subjects. Invest Ophthalmol Vis Sci 2012;53:1610–1616.

19. Lee EJ, Kim TW, Weinreb RN. Reversal of lamina cribrosa displacement and thickness after trabeculectomy in glaucoma. Ophthalmology 2012;119:1359–1366.

20. Tezel G, Trinkaus K, Wax MB. Alterations in the morphology of lamina cribrosa pores in glaucomatous eyes. Br J Ophthalmol 2004;88:251–256.

21. Torti C, Povazay B, Hofer B, Unterhuber A, Caroll J, Ahnelt PK, Drexler W. Adaptive optics optical coherence tomography at 120,000 depth scans/s for non-invasive cellular phenotyping of the living human retina. Opt Express 2009;17:19382–19400.

22. Spaide RF, Koizumi H, Pozzoni MC. Enhanced depth imaging spectral-domain optical coherence tomography. Am J Ophthalmol 2008;146:496–500.

23. Hughes DI, Duck FA. Automatic attenuation compensation for ultrasonic imaging. Ultrasound Med Biol 1997;23:651–664.

24. Foin N, Mari JM, Davies JE, Di Mario C, Girard MJ. Imaging of coronary artery plaques using contrast-enhanced optical coherence tomography. Eur Heart J Cardiovasc Imaging 2013;14:85.

25. Zimmo L, Strouthidis NG, Mari JM, Girard MJ. Contrast enhancement in images of the glaucomatous human optic nerve head (ONH) captured with enhanced depth imaging (EDI) optical coherence tomography (OCT). ARVO Meeting Abstracts 2012;53:2822.

26. Fatehee N, Yu PK, Morgan WH, Cringle SJ, Yu DY. The impact of acutely elevated intraocular pressure on the porcine optic nerve head. Invest Ophthalmol Vis Sci 2011;52:6192–6198.

27. Fatehee N, Yu PK, Morgan WH, Cringle SJ, Yu DY. Correlating morphometric parameters of the porcine optic nerve head in spectral domain optical coherence tomography with histological sections. Br J Ophthalmol 2011;95:585–589.

28. Strouthidis NG, Fortune B, Yang H, Sigal IA, Burgoyne CF. Longitudinal change detected by spectral domain optical coherence tomography in the optic nerve head and peripapillary retina in experimental glaucoma. Invest Ophthalmol Vis Sci 2011;52:1206–1219.

29. Ivers KM, Li C, Patel N, Sredar N, Luo X, Queener H, et al. Reproducibility of measuring lamina cribrosa pore geometry in human and nonhuman primates with in vivo adaptive optics imaging. Invest Ophthalmol Vis Sci 2011;52:5473–5480.

30. Agoumi Y, Sharpe GP, Hutchison DM, Nicolela MT, Artes PH, Chauhan BC. Laminar and prelaminar tissue displacement during intraocular pressure elevation in glaucoma patients and healthy controls. Ophthalmology 2011;118:52–59.

31. Burgoyne CF, Downs JC, Bellezza AJ, Suh JK, Hart RT. The optic nerve head as a biomechanical structure: a new paradigm for understanding the role of IOP-related stress and strain in the pathophysiology of glaucomatous optic nerve head damage. Prog Retin Eye Res 2005;24:39–73.